Two-State Models for Propylene Polymerization Using Metallocene Catalysts. 2. Application to ansa-Metallocene Catalyst Systems

ARTICLE *in* MACROMOLECULES · MAY 2001

Impact Factor: 5.8 · DOI: 10.1021/ma0021186

4 AUTHORS, INCLUDING:

Marcio Nele
Federal University of Rio de Janeiro
112 PUBLICATIONS **915** CITATIONS
SEE PROFILE

Muqtar Mohammed
University of Waterloo
4 PUBLICATIONS **122** CITATIONS
SEE PROFILE

Scott Collins
104 PUBLICATIONS **4,515** CITATIONS
SEE PROFILE

Articles

Two-State Models for Propylene Polymerization Using Metallocene Catalysts. 2. Application to *ansa*-Metallocene Catalyst Systems

Marcio Nele,[†] Muqtar Mohammed, Shixuan Xin, and Scott Collins*,[‡]

Department of Chemistry, University of Waterloo, 200 University Avenue West, Waterloo, Ontario, Canada N2L 3G1

Marcos L. Dias

Instituto de Macromoléculas Eloísa Mano/IMA, Universidade Federal do Rio de Janeiro, Cidade Universitária - CP: 68502, Rio de Janeiro 21945−970 RJ, Brasil

J. C. Pinto

Programa de Engenharia Química/COPPE, Universidade Federal do Rio de Janeiro, Cidade Universitária - CP: 68502, Rio de Janeiro 21945−970 RJ, Brasil

Received December 12, 2000; Revised Manuscript Received April 4, 2001

ABSTRACT: A kinetic model to describe the propylene polymerization behavior of *ansa*-metallocene catalysts was derived. The model can predict *n*-ad stereosequence distributions, polymer crystallinity, and related properties as well as distinguish between extremes in kinetic behavior expected for such catalysts. In particular, where polymer microstructure is sensitive to changes in $[C_3H_6]$, the model can provide reliable estimates of kinetic parameters of interest, including ratios between rates of some of the significant reaction steps involved in polymer microstructure formation. The model is applied to a description of the polymerization behavior of some simple symmetrical $[Me_2C(Cp)(Flu)MCl_2$; M = Zr, Hf] and unsymmetrical $[Me_2Y(Cp)(Ind)MCl_2$; M = Zr, Hf; Y = C, Si] *ansa*-metallocene catalysts, activated with methyl aluminoxane. With the former two catalysts, the Zr catalyst operates very close to the kinetic quenching limit where chain inversion (or chain back-skip) is slow compared to monomer insertion, while for the Hf analogue, these two processes have more comparable rates. In the more complicated, unsymmetrical systems, both Zr- and Hf-based systems (Y = Si) operate under conditions where inversion is much faster that propagation, whereas for the Hf catalyst (Y = C), intermediate behavior is observed, and the corresponding Zr complex (Y = C) produces poly(propylene) where propagation is faster than inversion.

Introduction

There is considerable interest in the study of metallocene catalysts which can exist in more than one state during polymer chain growth, particularly in the context of propylene polymerization.[1] Two basic types of metallocene catalysts that can display such behavior have been studied and can be classified as "bridged" or "fluxional". Depending on structure and polymerization conditions, the former class of catalysts can exhibit a wide range in behavior in propylene polymerization, producing poly(propylene) (PP) with predominantly isotactic[2] or syndiotactic[3] microstructures, as well as intermediate "forms" such as hemi-isotactic,[4] or elastomeric, stereo-block PP.[5] With some of these complexes the PP microstructure is sensitive to the nature of the counterion,[6] as well as solvent polarity,[7] while for others, such behavior is less evident.

In this paper, we attempt to reconcile such diverse behavior of bridged or *ansa*-metallocene catalysts through the development of a general kinetic model, which we believe will be applicable to all such systems, and which can be used to deduce the fundamental behavior of individual catalysts, through studies of their response to changes in polymerization conditions.[8]

The basic concepts behind the model developed here have been discussed elsewhere,[9] but will be reiterated here for sake of completeness. In essence, for a two-state, *ansa*-metallocene catalyst, there are two ways in which the states may interconvert, through the process of olefin insertion or via inversion at the metal center (e.g., Scheme 1, bridging group not shown for clarity).

This inversion process or chain back-skip as it is also known, was first invoked by Ewen and co-workers to explain the presence of the unique, *rmrr* pentad in the microstructure of s-PP produced using the prototypical, C_s-symmetric, *ansa*-metallocene $Me_2C(Cp)(Flu)ZrCl_2$, activated by MAO.[3a] Under the conditions studied, this inversion process must be slow relative to the (identical) rates of insertion from each (enantiomeric) state to account for the formation of predominantly s-PP by an alternating insertion mechanism.

The concept of chain inversion was also studied using unsymmetrical systems $Me_2C(3\text{-}RCp)(Flu)ZrCl_2$ (R =

[†] Present address: Programa de Engenharia Química/COPPE, Universidade Federal do Rio de Janeiro, Rio de Janeiro, Brazil.
[‡] Present address: Department of Polymer Science, University of Akron, Akron, OH 44325-3909.

10.1021/ma0021186 CCC: $20.00
Published on Web 05/11/2001

Scheme 1

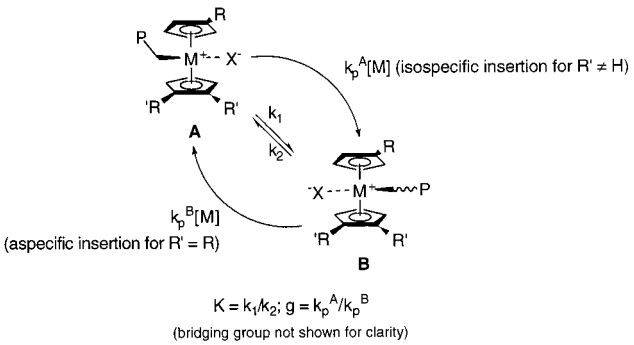

Me,[4a] ^{t}Bu[10]). In the former case (R = Me), hemi-isotactic PP was produced, one of the states being isospecific and the other aspecific indicating, that under the conditions studied, similar behavior, i.e., alternating insertion, may be invoked. However, in the latter case (R = ^{t}Bu), i-PP was formed as both states, though different, are isospecific with similar preferences for, e.g., the *re* face of coordinated monomer. Here it is less evident whether alternating insertion pertains; an equally valid explanation for the behavior seen is that only one state is involved in monomer insertion (as it is much more stable/reactive than the other state) and that the states are fully equilibrated prior to each insertion.[3c,9a]

As we have pointed out elsewhere, if the mechanism depicted in Scheme 1 is valid for all *ansa*-metallocene catalysts, then the microstructure of PP using either C_s- or C_1-symmetric complexes should be sensitive to changes in [C_3H_6] as interconversion between states via inversion *may* not depend on this variable.[9,11] Having said that, we and others[12] have observed this behavior with some, but not all types, of *ansa*-metallocene catalysts; clearly, what would be useful is a predictive and *quantitative* model based on the kinetics of the process shown in Scheme 1 to strengthen and/or refute this hypothesis.

In developing a quantitative model for the mechanism shown in Scheme 1 and applying it to a description of polymer microstructure (or other experimental observable), there are two basic approaches that can be adopted.

A probabilistic approach would involve defining probabilities for each elementary reaction step available to a given state, weighting these appropriately using a parameter proportional to the probability of a particular state being involved in polymerization, and using all of these parameters to model, e.g., pentad distributions. Such models have already been developed and used to describe the polymer microstructure for PP prepared using complexes of this type.[13]

A most recent version of this type of model invokes three parameters α (the stereoselectivity of insertion at state A), β (the analogous parameter for state B), and γ, where the latter parameter, can be defined in terms of the elementary steps summarized in Scheme 1 as $\gamma = k_1[A]/(k_1[A] + k_p^A[A][M]) = k_1/(k_1 + k_p^A[M])$ and represents the probability of chain back-skip for, e.g., state A.[14] It is obvious that γ is actually a variable in that it *may* be dependent on [M]. Furthermore, in the general case, one needs an additional variable δ in that chain back-skip from B can occur with a different probability than from state A if A ≠ B.[13]

These models can accurately reproduce pentad distributions at different [M] but the relationship of all of the parameters used to the elementary steps outlined in Scheme 1 may not be obvious except when the states A and B are the same or related by mirror symmetry.

Further, different values of the parameters might be obtained from modeling of (different) pentad distributions of polymer formed under different experimental conditions (e.g., at different [M]). As we will show here, the intrinsic parameters that can be used to describe the behavior of such systems should not show variation with experimental conditions and moreover, some parameters may be correlated with each other. If this is not taken into account using a probabilistic (or any) model, the estimates of the parameters obtained may not be chemically meaningful.

An alternative approach treats formation of, e.g., stereo-sequences as a kinetic event and explicitly solves or numerically evaluates the relevant differential equations. These kinetic models have been widely used to describe the broad MW or composition distributions in polymers or copolymers produced using Ziegler−Natta catalysts, but are less frequently used to model stereosequence distributions, in part because of their mathematical complexity.[15]

We have used a kinetic approach to describe pentad, MW, crystallinity and isotactic/atactic sequence length distributions for polymers prepared using two-state, *ansa*-metallocene catalysts for several reasons. The parameters employed in the modeling are directly (and clearly) related to the mechanism outlined in Scheme 1; thus extraction of fundamental quantities of interest (i.e., the rate constants or ratios of these) from, e.g., the pentad distribution and its response to changes in [M] should be more straightforward. Second, the kinetic approach is ideally suited to calculating sequence length distributions and these are of importance with respect to predictions of polymer crystallinity. Finally, the kinetic approach makes clear which parameters should be constant with respect to changes in experimental conditions and thus data obtained under different conditions may be used to provide more reliable estimates of these fundamental parameters, as well as distinguish between different (kinetic) models.

Results and Discussion

Model Definition. It is appropriate to define parameters of interest at the outset prior to discussing the model and its predictions. Polymer microstructure will be determined by several factors, one of which is the stereoselectivity of insertion (denoted by α and β) and mechanism of stereo-control for each state (e.g., enantiomorphic site vs chain-end control).[16] Although we illustrate the model assuming simple enantiomorphic site control for each state, all possible scenarios (site vs chain end vs mixed control for either or both states) have been treated.[17]

Additionally, the polymer microstructure will be controlled by the relative rates of insertion and inversion. We have defined a variable Δ that relates these two rates through eq 1, where Ψ is the mole fraction of

$$\Delta = \frac{(k_p^A[A] + k_p^B[B])[M]}{k_1[A] + k_2[B]} = \frac{[k_p^A\Psi + k_p^B(1-\Psi)]}{[k_1\Psi + k_2(1-\Psi)]}[M] \quad (1)$$

catalyst in state A with Ψ = [A]/([A] + [B]). Thus, Δ is related to [M] and as such represents an experimental

variable. The quantity Ψ can also be related to the rate constants etc. shown in Scheme 1 by

$$\Psi = \frac{k_p^B[M] + k_2}{k_p^B[M] + k_2 + k_p^A[M] + k_1} \quad (2)$$

Substitution of eq 2 (and the corresponding expression for $1 - \Psi$) into eq 1 gives

$$\Delta = \frac{(2k_p^A k_p^B[M] + k_2 k_p^A + k_1 k_p^B)}{(2k_1 k_2 + k_2 k_p^A[M] + k_1 k_p^B[M])}[M] \quad (3)$$

Factoring out $k_1 k_p{}^B$ from numerator and denominator and with reference to Scheme 1, using the expressions $g = k_p^A/k_p^B$ (which represents the intrinsic reactivity difference between the two states) and $K = k_1/k_2$ (which describes the intrinsic stability difference between the two states) we obtain after some algebra

$$\Delta = \frac{2(k_p^B/k_2)(g/K)[M] + (g/K + 1)}{(g/K + 1)[M] + (2k_2/k_p^B)}[M] \quad (4)$$

If we define $\delta = k_p^B/k_2$ as the ratio of the rate constants of insertion to inversion for *one* of the states (in this case B) we finally obtain

$$\Delta = \frac{2(g/K)\delta[M] + (g/K + 1)}{(g/K + 1)\delta[M] + 2}\delta[M] \quad (5)$$

Thus, Δ is a function of two fundamental quantities in addition to [M]. From a modeling perspective, g/K and δ are two of the four independent parameters (the others being α and β) that are varied to describe, e.g., pentad distributions, and Δ may be calculated from these quantities using eq 5 at any particular [M]. The lumped parameter g/K can be interpreted as a parameter describing the relative contribution of each state to chain growth. Since a change in the relative stability of the two states (K), has the same effect on polymer microstructure as a change in their intrinsic reactivity (g), g/K is the only parameter that can be unequivocally extracted from, e.g., modeling of pentad distributions; determination of K thus requires independent knowledge of g or vice versa. It is worthwhile to note that K is only related to the steady-state concentrations of states A and B (i.e., K = [B]/[A], Scheme 1) when the states are fully equilibrated by the inversion process prior to each monomer insertion.

The total number of parameters used in the kinetic model (i.e., α, β, δ, and g/K) is obviously the same as in, e.g., the probabilistic model developed by Farina and co-workers.[13] Here, it is clear what relationship the model parameters have to the proposed mechanism depicted in Scheme 1 and that *none* of them should change with varying [M] (i.e., only Δ will change as it is a function of [M]).

Model Description. The elementary steps involved in polymer chain formation and termination are given in Table 1; we have assumed that chain growth follows first-order kinetics in [C_3H_6] but other kinetic orders (or states needed to describe other kinetic orders)[1b] can be invoked without difficulty. Here the superscript (A or B) denotes the state involved; for example k_p^A and k_{trh}^A are the rate constants for propagation and chain-transfer (via β-hydrogen elimination), respectively from state A.

A similar approach was adopted for the kinetic formation of dyad stereo-sequences using the fundamental processes outlined in Table 2; here, for example, k_{AR} is the rate constant for formation of a RR-dyad from state A with $\alpha = k_{AR}/(k_{AR} + k_{AS})$. Although dyads are of less utility than longer stereo-sequences in the description of polymer microstructure, this approach can be extended to n-ads of any composition/length.

Table 1. Kinetics of Chain Growth Using a Two-State *ansa*-Metallocene Complex[a]

propagation	$P_n^A + M \xrightarrow{k_p^A} P_{n+1}^B$
	$P_n^B + M \xrightarrow{k_p^B} P_{n+1}^A$
chain transfer	$P_n^A + M \xrightarrow{k_{tm}^A} Q_n + P_1^B$
	$P_n^A (+M) \xrightarrow{k_{th}^A} Q_n + P_1^B$
	$P_n^B + M \xrightarrow{k_{tm}^B} Q_n + P_1^A$
	$P_n^B (+M) \xrightarrow{k_{th}^B} Q_n + P_1^A$
inversion	$P_n^A \xrightarrow{k_1} P_{n+1}^B$
(Scheme 1)	$P_n^B + M \xrightarrow{k_2} P_n^A$

[a] P_n^i is a living polymer chain in the state i (i = A, B) of length n while Q_n is a dead polymer chain of length n.

Table 2. Formation of Dyad Stereosequences Using a Two-State *ansa*-Metallocene Catalyst[a]

propagation from state i	$Zr_{RR}^i + R \xrightarrow{kir} Zr_{RR}^j + RR$
(i, j = A, B, and i ≠ j)	$Zr_{RR}^i + S \xrightarrow{kis} Zr_{SR}^j + RR$
	$Zr_{RS}^i + R \xrightarrow{kir} Zr_{RR}^j + RS$
	$Zr_{RS}^i + S \xrightarrow{kis} Zr_{SR}^j + RS$
	$Zr_{SR}^i + R \xrightarrow{kir} Zr_{RS}^j + SR$
	$Zr_{SR}^i + S \xrightarrow{kis} Zr_{SS}^j + SR$
	$Zr_{SS}^i + R \xrightarrow{kir} Zr_{RS}^j + SS$
	$Zr_{SS}^i + S \xrightarrow{kis} Zr_{SS}^j + RR$
inversion (Scheme 1)	$Zr_R^A \underset{k_2}{\overset{k_1}{\rightleftharpoons}} Zr_R^B$
	$Zr_S^A \underset{k_2}{\overset{k_1}{\rightleftharpoons}} Zr_S^B$
	$Zr_{RR}^A \underset{k_2}{\overset{k_1}{\rightleftharpoons}} Zr_{RR}^B$
	$Zr_{RS}^A \underset{k_2}{\overset{k_1}{\rightleftharpoons}} Zr_{RS}^B$
	$Zr_{SR}^A \underset{k_2}{\overset{k_1}{\rightleftharpoons}} Zr_{SR}^B$
	$Zr_{SS}^A \underset{k_2}{\overset{k_1}{\rightleftharpoons}} Zr_{SS}^B$

[a] $Zr_{RS}^i + R \xrightarrow{kir} Zr_{RR}^j + RS$ represents formation of state j (j = A, B) bearing a new RR-dyad and production of a RS-dyad on the polymer chain, via insertion of monomer by its *re* face (denoted R) at a state i (i ≠ j) bearing an R,S-dyad. Note that the newly formed RR-dyad shares an R-configured monomer unit with the previous dyad.

Table 3. Formation of Isotactic Sequences Using a Two-State, *ansa*-Metallocene Complex[a]

propagation	$Zr^{A}_{R_i} + R \xrightarrow{kar} Zr^{B}_{R_i+1}$
	$Zr^{A}_{R_i} + S \xrightarrow{kas} Zr^{B}_{S_i} + r_i$
	$Zr^{A}_{S_i} + R \xrightarrow{kar} Zr^{B}_{R_1} + s_i$
	$Zr^{A}_{S_i} + S \xrightarrow{kas} Zr^{B}_{S_i+1}$
	$Zr^{B}_{S_i} + R \xrightarrow{kbr} Zr^{A}_{R_i+1}$
	$Zr^{B}_{R_i} + S \xrightarrow{kbs} Zr^{A}_{S_i} + r_i$
	$Zr^{B}_{S_i} + R \xrightarrow{kbs} Zr^{A}_{R_i} + s_i$
	$Zr^{B}_{S_i} + S \xrightarrow{kbs} Zr^{A}_{S_i+1}$
inversion (Scheme 1)	$Zr^{A}_{R_i} \underset{k_2}{\overset{k_1}{\rightleftharpoons}} Zr^{B}_{R_i+1}$
	$Zr^{A}_{S_i} \underset{k_2}{\overset{k_1}{\rightleftharpoons}} Zr^{B}_{S_i}$

[a] $Zr^{A}_{R_i} + S \xrightarrow{kis} Zr^{B}_{S_i} + r_i$ represents the formation of an isotactic block of R-configured monomer units of length i (r_i) and catalyst in state B bearing a "living" S-configured, isotactic block of unit length, by insertion of monomer via its S_i face (S) from catalyst in state A bearing a "living" isotactic sequence of length i.

Finally, the formation of, e.g., isotactic blocks can be treated as a kinetic event provided a different scheme is used which is independent of the nature of the states involved in the formation of a stereo-block (Table 3).[8] In this table, $Zr^{A}_{R_i}$ is a polymer chain bearing an isotactic sequence of R-configurated monomer units of length i in the state A.

The differential equations describing these processes and their solution rely on the assumption of quasi-steady states and the principle of mass balance on each of the species present; the derivation of the various expressions governing molecular weight or stereosequence distributions is not compact and the details are presented in the Supporting Information. Here, we focus on the model predictions of experimental behavior and how they relate to the fundamental parameters previously identified (Scheme 1).

It is perhaps appropriate to point out that the mechanism proposed for the polymerization process is the *simplest* one that can be invoked.[18] Subtle, but nevertheless important, issues such as the likelihood that states generated, following a stereo- or regioirregular propylene insertion, would have, e.g., different k_p/k_{tr} characteristics (or even different values of α and β for a subsequent insertion) are not considered.[1] Indeed it will become obvious that for many practical situations, even this simple model will have more parameters than can be uniquely extracted from an analysis of pentad distributions; knowledge of defect structures and their response to changes in polymerization conditions[1] may allow the use of more sophisticated versions of this model.

Model Predictions. Stereosequence Distributions. In Figure 1 the calculated response of the *mmmm* pentad intensity to changes in Δ is shown for various values of g/K with the A state isospecific ($\alpha = 1.0$) and B aspecific ($\beta = 0.5$). The behavior is intuitive; for low values of Δ (i.e., chain inversion much faster than insertion) Curtin−Hammett (C−H) conditions pertain,

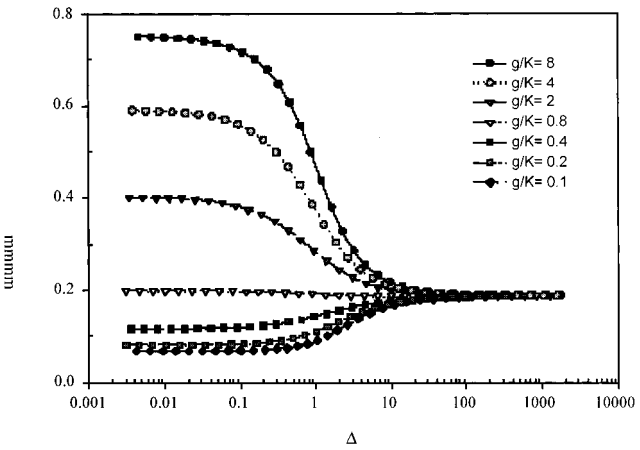

Figure 1. Normalized intensity of the mmmm pentad vs Δ for different values of g/K, of PP produced with a two-state, *ansa*-metallocene catalyst ($\alpha = 1.0$, $\beta = 0.5$).

the pentad distribution is invariant to limited changes in Δ (i.e., [M]) and the PP will be predominantly isotactic if $g/K \gg 1$ or atactic if the converse is true. For $\Delta \gg 1$, kinetic quenching (KQ) conditions (i.e., perfectly alternating insertion) prevail, the *mmmm* pentad intensity converges to the same limit for all values of g/K, the overall pentad distribution corresponds to hemi-isotactic PP (with % *mmmm* = 18.75 for the values of α and β selected) and the pentad distribution is again invariant to further increases in Δ. If $g/K = 1$, then *mmmm* does not change with Δ and polymer with a *mmmm* pentad intensity corresponding to hemi-isotactic PP would be produced under all conditions; fortunately, the intensities of some the other pentads are different in the two, limiting regimes, and thus one can distinguish from the complete pentad distribution in this situation whether a catalyst operates under C−H or KQ conditions (except in the trivial case where $\alpha \approx \beta$).

In the C−H regime ($\Delta \ll 1$), the rate of chain inversion is much faster than insertion (for both states), the final pentad distribution is similar to that resulting from a Bernoullian trial as the two state catalyst behaves like a single-state catalyst, and the only parameter that can be uniquely obtained by nonlinear regression analysis of the pentad distribution is the average stereoselectivity of monomer incorporation given by[9a]

$$\bar{\epsilon} = \frac{\alpha(g/K) + \beta}{g/K + 1} \tag{6}$$

Under these conditions the fundamental parameters of interest (g/K, α, β and δ) are highly correlated as an absolute range of values for Δ cannot be readily determined − in essence one could be operating anywhere along the horizontal axis as a function of [M] (Figure 1) as long as $\Delta \ll 1$, and thus g/K and δ (eq 5) cannot be determined by modeling of the pentad distribution.

In the KQ regime, the pentad distribution is a function of two parameters only (α and β); all the other kinetic information is lost and cannot be recovered from an analysis of the pentad distribution.

In principle, if one could go from C−H to KQ conditions with any particular catalyst by varying monomer concentration, unambiguous determination of all of the intrinsic parameters would be possible (Figure 1). That is, α and β could be uniquely determined from the pentad distribution in the KQ regime, while g/K would be available from the corresponding analysis under

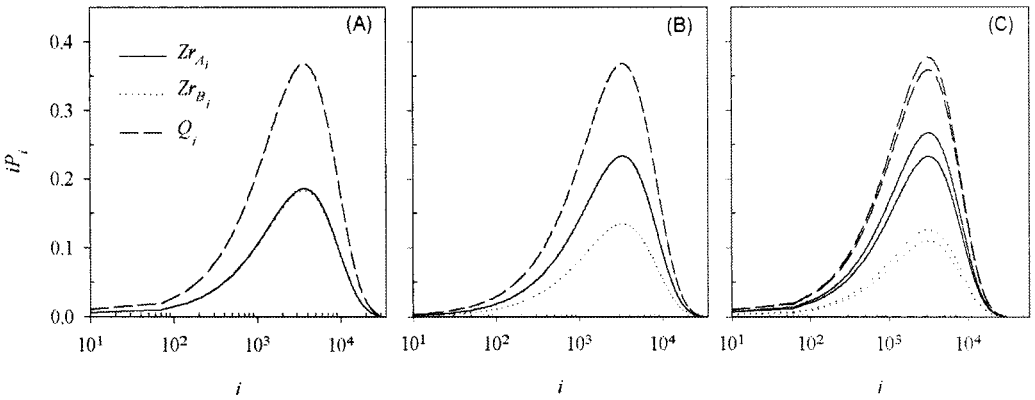

Figure 2. Calculated molecular weight distributions of living (Zr_A, Zr_B) and dead (Q_n) polymer chains of PP produced with a two-state, *ansa*-metallocene catalyst under (a) Curtin−Hammett (DP_n = 3665) (b) intermediate (DP_n = 3314) and (c) kinetic quenching conditions (DP_n = 3189) with $K = 1.0$, $g = k_p^A/k_p^B = 0.47$; $k_p^B = 403\ M^{-1}\ h^{-1}$; $k_{tm}^A = k_{tm}^B = 0.081\ M^{-1}\ h^{-1}$; $k_{th}^A = k_{th}^B = 0$; $[C_3H_6] = 1.0$ M; $k_p^B/k_{tm}^B = 4981$ and $k_p^A/k_{tm}^A = 2346$.

C−H conditions, the absolute position of the curve along the horizontal axis additionally being influenced by δ (see eq 5). The minimum requirement for estimation of all of these parameters is variation of the pentad distribution with monomer concentration and, ideally, the observation of asymptotic behavior with increasing [M] is needed for unambiguous determination. That is, both slope in the intermediate kinetic regime ($\Delta \sim 1$) and curvature, as one approaches, e.g., KQ conditions, serve to uniquely define α, β, g/K, and δ.

It is important to emphasize what changes in Δ are required to observe a significant change in the pentad distribution as a function of [M]. Evidently, one should expect dramatic changes only when g/K differs significantly from 1; even so, Figure 1 illustrates that Δ must vary by at least 10^2-10^3 in order to go from C−H to KQ conditions with any particular catalyst. This requirement is essentially impractical for any given catalyst at a particular temperature − propene concentration can only be easily varied from about 1−11 M at 25 °C and thus changes in Δ are restricted (experimentally) to about 10 units.[19]

Thus, many *ansa*-metallocene complexes may not show variation of the PP pentad distribution with [M] and the modeling of polymer microstructure for these cases should reveal which of the two kinetic extrema (i.e., Curtin−Hammett vs kinetic quenching) is most probably involved. In situations where variation of the pentad distribution with [M] is observed, there may be significant correlation between model parameters (vide infra) and unambiguous determination of all parameters can require more information than is available from modeling of the pentad distribution.

The migratory insertion process has strong effects on the distribution of block lengths of polymer produced by each state. One feature that emerges is that a block with an average length of, e.g., five monomer units, used as working hypothesis in some modeling studies,[11b,20] will never be produced by *both* catalyst states under a given set of conditions. The maximum, average block length for a particular state [BL_I(max): I = A, B) is observed under C−H conditions (eqs 7 and 8). The fact that one state may be much more reactive/stable than the other one and is producing long blocks necessarily implies that the other state is producing very short blocks (in the limit with an average length close to one unit). If the states have similar reactivity/stability, the maximum average block length produced by both is only two monomer units long. Naturally, if the catalyst operates under KQ conditions, the block length produced by each state is only one unit long.

$$BL_A(\max) = 1 + g/K \tag{7}$$

$$BL_B(\max) = 1 + K/g \tag{8}$$

In summary, the model developed should accurately describe the microstructure of PP and thus the kinetic behavior of two-state, *ansa*-metallocene catalysts, given the fundamental assumptions involved (vide supra) but, as indicated above, extraction of detailed kinetic information from the pentad distributions requires caution and, in some cases, more data than available from polymerization experiments.

Molecular Weight Distribution. In the absence of catalyst degradation, mass-transfer effects or related processes, any two-state, *ansa*-metallocene complex should produce polymer with a MWD approximating a Schultz−Flory, most-probable distribution, with M_w/M_n never larger than 2. This is easily appreciated—the two states always interconvert during polymerization by either inversion or insertion (Scheme 1) on a time scale that is fast compared to the kinetic chain length (i.e., the rate of formation of "dead" polymer chains).

The MWD of both living and dead polymer chains, over the whole range of behavior expected for these types of catalysts is shown in Figure 2. Changing from the C−H to KQ regime has no effect on the breadth of the MWD of the dead polymer; however, the average degree of polymerization may be strongly influenced as the k_p/k_{tr} characteristics of each state are weighted differently in the two limiting regimes—under the C−H conditions one observes averaged behavior, depending on the magnitude of g/K, while under KQ conditions, the k_p/k_{tr} characteristics of the state most prone to chain transfer may dominate.

An unusual feature of the model that shows up under KQ conditions (i.e., strictly alternating insertion), are that there are separate distributions for living (and dead) chains derived from an even vs an odd number of insertions and thus double MWD curves appear in Figure 2C for both living and dead polymer chains.

This can be explained using simple probability arguments. For example, consider a situation in which the probability of chain growth from the A state is unity (i.e., $p_A = k_p^A/k_p^A + k_{tr}^A = 1$ where we assume exclusive

chain transfer to monomer for simplicity) while chain transfer can occur from the B state ($0 < p_B < 1$). For chains that initiate in the A state, it is easy to show that only "dead" chains of odd length will be produced while the converse is true for chains that initiate in the B state (i.e., only even length chains are allowed, eq 9). Furthermore, for this particular situation it is also clear that the number distribution of the odd length chains in the A state (x_n^A with n odd) is the same as that for the even length chains in the B state (x_n^B with n even).

$$x_n^A = x_A^{n/2}\, x_B^{n/2}(1 - p_A) = 0 \quad \text{if } p_A = 1 \text{ for } n = 2, 4, 6, \ldots$$

$$x_n^A = p_A^{(n+1)/2}\, p_B^{(n-1)/2}(1 - p_B) \neq 0 \quad \text{if } p_B \neq 1 \text{ for } n = 3, 5, 7, \ldots$$

$$x_n^B = p_A^{n/2}\, p_B^{n/2}(1 - p_B) \neq 0 \quad \text{if } p_B \neq 1 \text{ for } n = 2, 4, 6, \ldots$$

$$x_n^B = p_A^{(n+1)/2}\, p_B^{(n-1)/2}(1 - p_B) = 0 \quad \text{if } p_A = 1 \text{ for } n = 3, 5, 7, \ldots \quad (9)$$

In the more usual case where chain transfer can occur from both states but their k_p/k_{tr} characteristics are different (i.e., $0 < p_A \neq p_B < 1$), it can be appreciated from eq 9 that, e.g., the number distribution for even length chains that initiate in state A will differ from that of odd length chains. Further, the number distribution of odd (or even) length chains that initiate from state A will also differ from that of odd (or even) length chains that initiate from state B [by a factor of $(1 - p_A)/(1 - p_B)$], assuming an equal number of chains initiate from each state.

The dead chain length distributions depicted in Figure 2c were calculated by using the fraction of living chains present in each of the two different states [i.e. by $\Psi = k_p^B/(k_p^B + k_p^A) = 1/(1 + g)$ under KQ conditions, see eq 2]. This treatment ignores the more complex question as to how many chains actually initiate in the A vs the B state [which is probably $\neq \Psi$ for, e.g., the A state as the initiating species (e.g., M−H or M−^{n}Pr) are unlikely to be similar in their reactivity/stability differences as the two states involved in propagation].[18] Nevertheless, one would still obtain separate living and dead chain length distributions for odd vs even length chains that would be different if the two states differ in their k_p/k_{tr} characteristics.

From a practical perspective, one can ignore this feature as, for a high MW polymer, it is not usually possible to detect even vs odd length chains.[21] Moreover, it is evident from Figure 2C that both the average quantities and breadth of the chain length distributions are the same for even and odd length chains, whether living or dead.

Polymer Crystallinity. Another observable that relates to PP produced using two-state *ansa*-metallocene catalysts is polymer crystallinity. The phenomenon is related to the presence of long tactic sequences (i.e., isotactic or syndiotactic) in the whole polymer sample. In the case of elastomeric PP, the minimum (isotactic) sequence length that gives rise to crystallization in these materials was estimated at about 14 monomer units.[22]

The kinetic model developed here can be used to estimate the length distribution of isotactic blocks, and derived quantities like the average isotactic block length

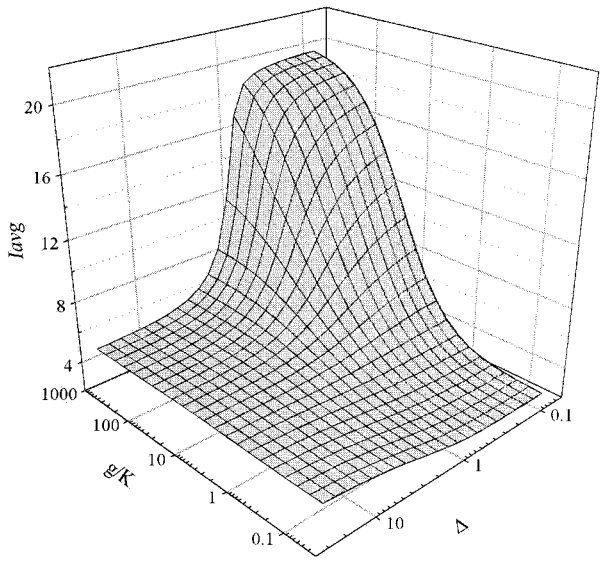

Figure 3. Effect of g/K and Δ upon I_{AVG}, the average isotactic sequence length ($\alpha = 0.95$, $\beta = 0.60$).

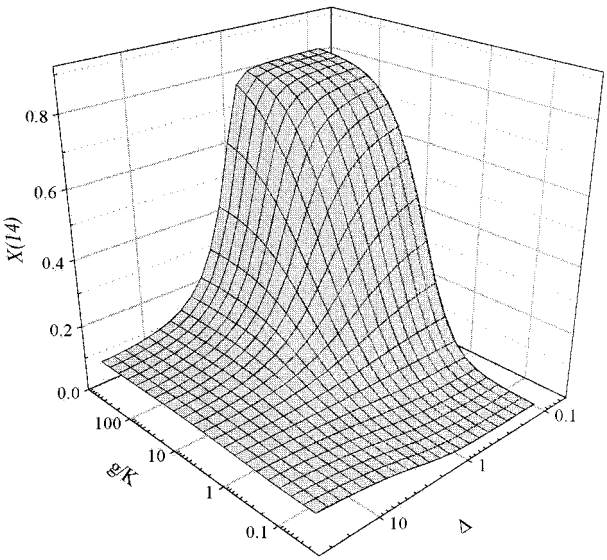

Figure 4. Effect of g/K and Δ upon $X(14)$, the mass fraction of isotactic blocks ≥ 14 units ($\alpha = 0.95$, $\beta = 0.60$).

(I_{AVG}), and the weight fraction of isotactic sequences larger than 14 monomer units [$X(14)$]. The latter estimate corresponds to an upper theoretical limit for whole polymer crystallinity; in conjunction with Monte Carlo techniques,[23] it can also be used to estimate the minimum crystallinity in these materials.

Figures 3 and 4 show the effect of g/K and Δ on I_{AVG}, and on $X(14)$. From Figure 3 it should be clear that unless the isospecific state is significantly more stable/reactive than the aspecific site, I_{AVG} is very small. In fact, if $g/K \approx 1$, $I_{AVG} \sim 5$ monomer units long. An interesting consequence of this finding is that the relationship $N_{ISO} = 4 + 2[mmmm]/[mmmr]$, which is often used to estimate the average length of isotactic blocks (with $N_{ISO} \geq 4$) from pentad distribution data, can give rise to misleading information, since a significant fraction of the actual isotactic block length distribution may be ≤4 units long and even the average length may be ≤4.

In Figure 4, it should be pointed out that only a small region of the complete surface would likely correspond to the formation of elastomeric PP. If the catalyst

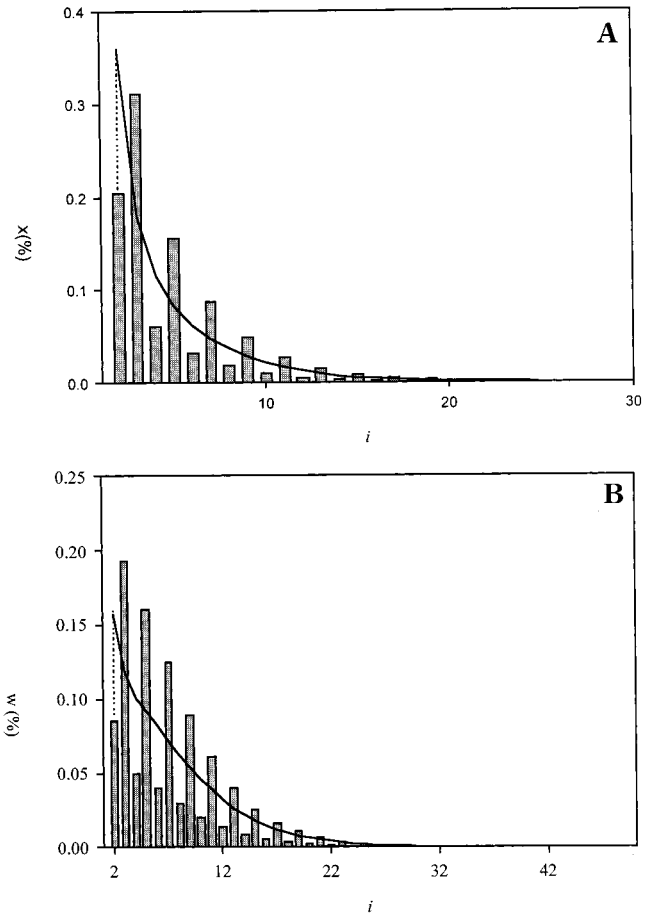

Figure 5. (A) Number-average and (B) weight-average isotactic sequence length distributions for PP produced by a two-state *ansa*-metallocene catalyst with $\Delta \gg 1$ (vertical bars) and $\Delta \ll 1$ (continuous curve) ($\alpha = 1.0$, $\beta = 0.5$, $g/K = 1.0$).

operates (only) under KQ conditions, the crystallinity will possibly be too low, and the polymer could be amorphous. In the C−H regime, if one of the states is much more stable/reactive than the other one, the polymer will have a too high ($g/K \gg 1$) or too low ($g/K \ll 1$) a crystallinity to exhibit elastomeric properties.

As well, $X(14)$ and I_{AVG} are very sensitive functions of the values of g/K and Δ and for any particular values of α and β if the isospecific state is more reactive/stable. These features have important consequences in the design of (and under what conditions) *ansa*-metallocene catalysts will be useful for the synthesis of elPP, since only a small range of fundamental catalyst parameters give rise to materials with intermediate crystallinity necessary for elastomeric properties.

In Figure 5, parts A and B, we compare the normalized, number and weight-average, isotactic block length distributions of polymer samples produced under C−H and KQ conditions by an *ansa*-metallocene with a perfectly isospecific state ($\alpha = 1.0$) and an perfectly aspecific site ($\beta = 0.5$) with $g/K = 1$. The distribution produced under C−H conditions is very narrow and homogeneous. However, the distribution produced under KQ conditions, although narrow, shows peculiar heterogeneity.

This odd behavior is related to simple probability arguments that pertain to alternating insertion. It is easy to see that isotactic blocks will always end with insertion from the aspecific state (B) if $\alpha = 1$ (i.e., a misinsertion from the A state is not allowed). Because of the alternating insertion pattern, isotactic sequences of, e.g., length 3 must then have initiated in state A, while isotactic sequences of length 2 must have initiated in state B. The former sequence corresponds to a *mmr* tetrad while the latter corresponds to a *mr* triad. It can be shown that the numerical values of the probability of these two stereo-sequences are equal when $\alpha = 1$, and are at least comparable when α is close to 1, for a site control model and alternating insertion.

The number distribution of isotactic sequences calculated using the kinetic model (Figure 5A) does not exhibit the exact behavior predicted by simple probability arguments, because the latter approach only gives results that are meaningful when sequences of the *same* length are compared. In any event, it should be self-evident that there are separate distributions for odd vs even length sequences in a manner entirely analogous to that observed for the MWD of living chains (vide supra). Note that the average of the odd and even length isotactic sequence distributions is the same as that observed under C−H conditions since $g/K = 1$ in Figure 5.

Model Application to C_s *ansa*-Metallocene Catalysts. The simplest, two-state *ansa*-metallocene catalysts that can be treated by the model are those where the states are related by symmetry. For example, for the catalyst derived from $Me_2C(Cp)(Flu)MCl_2$ (M = Zr, and Hf—**1** and **2**, respectively), it is immediately evident that $g = K = 1$ and that α and β have the same magnitude but are of opposite sign (i.e., $\alpha = 1 - \beta$ in absolute terms).

These catalysts were selected for further study because they have been previously studied by others[3,24] and different behavior is observed in liquid propylene, with the Hf catalyst being less active and producing a less stereoregular polymer. Others have suggested this latter feature is only due to a decrease in the intrinsic stereoselectivity of insertion; while this may be correct, it is important to recognize that these catalysts may be operating over different ranges in Δ (which would also lead to differences in the pentad distribution).

Shown in Table 4 are the experimental (and some calculated) pentad distributions for both catalysts, activated by MAO, as a function of $[C_3H_6]$ from 1 to 10 M (i.e. liquid propylene), and in Table 5 the estimated values for $\Delta/[M]$ and α (with $g/K = 1$) as well as the agreement between calculated and observed results are depicted.

In Figure 6 is shown the response of the *rmrr* pentad to changes in Δ for both catalysts. While the main pentads relating to s-PP do not change significantly with $[C_3H_6]$ for the Zr catalyst (Table 4), the unique *rmrr* pentad corresponding to chain back-skip does vary and allows one to place both catalysts on the same master curve in terms of Δ. The estimated average stereoselectivity was $\alpha = 0.95$ for the Hf and $\alpha = 0.98$ for the Zr catalyst (Table 5) at 30 °C.

Evidently, the different behavior observed for Hf vs Zr under the same experimental conditions can be explained invoking differences in the stereoselectivity of insertion, however it seems that differences in the catalyst operating regime are as important. The fact that the pentad distribution for the PP produced using the Hf catalyst varies significantly with changes in $[C_3H_6]$ while that for Zr does not serves to indicate that the two catalysts operate under different kinetic regimes, but are otherwise quite similar.

Table 4. Polymerization of Propylene Using $Me_2C(Cp)(Flu)MCl_2$ and PMAO[a]

							pentad distribution[c]				
entry	M	T (°C)	[M]	$M_w \times 10^3$	PD	A[b]	*rmmr*	*mmrr*	*xmrx*	*rrrr*	*rrrm*
1	Zr	30	0.9	132	1.8	7.7	0.02 (0.02)	0.04 (0.04)	0.03 (0.03)	0.85 (0.85)	0.06 (0.06)
2	Zr	30	1.8	130	1.7	12.1	0.02 (0.02)	0.03 (0.03)	0.03 (0.03)	0.89 (0.89)	0.04 (0.04)
3	Zr	30	10.5[d]	159	1.8	19.6	0.02 (0.02)	0.03 (0.03)	0.02 (0.02)	0.90 (0.90)	0.04 (0.04)
4	Zr	40	1.4	110	1.7	8.4	0.02	0.03	0.04	0.85	0.04
5	Zr	40	10.3[d]	123	2.5	50.3	0.02	0.04	0.02	0.88	0.04
6	Zr	50	0.9	86	1.9	4.9	0.02	0.04	0.04	0.83	0.08
7	Zr	50	1.8	87	1.8	10.9	0.02	0.03	0.03	0.87	0.06
8	Zr	50	9.8[d]	114	2.1	95.7	0.02	0.04	0.02	0.87	0.06
9	Hf	30	0.9	913	2.0	0.6	0.04 (0.04)	0.08 (0.08)	0.05 (0.06)	0.68 (0.67)	0.12 (0.12)
10	Hf	30	1.8	968	2.0	1.4	0.04 (0.04)	0.08 (0.08)	0.04 (0.04)	0.69 (0.71)	0.12 (0.11)
11	Hf	30	10.5[d]	1080	1.7	6.4	0.03 (0.04)	0.06 (0.08)	0.04 (0.02)	0.74 (0.75)	0.12 (0.09)
12	Hf	40	1.4	886	1.9	3.3	0.04	0.06	0.04	0.75	0.12
13	Hf	40	10.3[d]	915	2.0	13.0	0.04	0.08	0.05	0.69	0.14
14	Hf	50	0.9	666	2.1	3.5	0.04	0.08	0.09	0.63	0.13
15	Hf	50	1.8	697	1.9	8.8	0.04	0.07	0.06	0.68	0.14
16	Hf	50	9.8[d]	725	2.2	16.0	0.03	0.06	0.03	0.76	0.09

[a] Polymerization conditions: Toluene solvent (0.75 L), Al:M ~ 1000:1, [M] = 2.5−5.0 μM, 1000 rpm except where noted. [b] Activity in 10^6 g of PP/mol of M × h. [c] Experimental pentad intensities with calculated values in parentheses for entries 1−3 and 9−11. [d] Experiments in liquid propylene with Al:M ~ 3000:1 and catalyst/cocatalyst introduced in a small volume (ca. 20 mL total) of toluene.

Table 5. Calculated Parameters and Fits of the Model to Pentad Distributions for $Me_2C(Cp)(Flu)MCl_2$[a]

entry	M	T (°C)	Δ/[M][b]	α[c]	RSS (10^{-3})[d]
1	Zr	30	75	0.98_1	0.72
2	Zr	40	60	0.97_9	0.84
3	Zr	50	48	0.97_7	0.78
4	Hf	30	35	0.94_8	2.32
5	Hf	40	27	0.94_8	2.10
6	Hf	50	22	0.94_8	1.28

[a] For experimental and some representative, calculated pentad distributions see Table 4. [b] This parameter = $\delta = k_p/k_1$ for C_s-symmetrical complexes. [c] Both states have the same value of α but of opposite sign. [d] This represents the residual sum of squares between calculated and observed pentad intensities over all experiments conducted at constant T but different [M] (see Table 4).

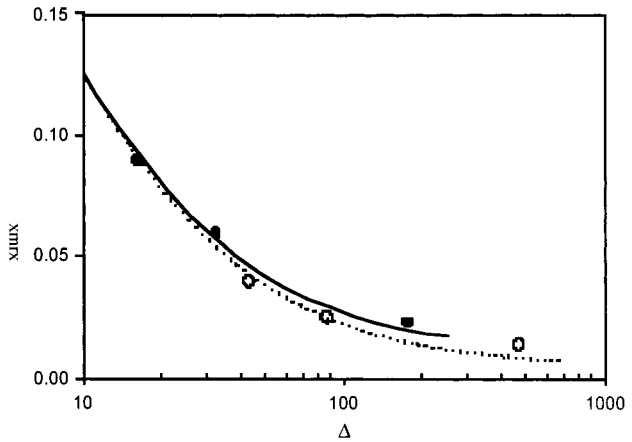

Figure 6. Theoretical fits and *xmrx* pentad intensities (normalized to unity) vs Δ for s-PP prepared with $Me_2C(Cp)$-$(Flu)HfCl_2$/MAO (—) and $Me_2C(Cp)(Flu)ZrCl_2$/MAO (···) catalysts at 50 °C.

With these simple catalysts, it is instructive to examine temperature-dependent behavior. Changes to the pentad distribution as a function of temperature could result from changes in α and/or changes in Δ/[M] which in this case is given by $k_p^A/k_1 = k_p^B/k_2$. A series of polymerization experiments over the temperature range 30−50 °C and at different monomer concentrations were conducted using both catalysts and the results are summarized in Table 4, while the best estimates of α and Δ/[M] at each temperature are shown in Table 5. For both Zr and Hf complexes, α seems largely temperature independent (or more precisely our data and the fit of the model to the data does not allow accurate enough prediction of α at the different temperatures) while a meaningful temperature dependence for Δ/M was noted. Eyring plots of ln(Δ/[M]) vs $1/T$ were linear and the following activation parameters were obtained:

M	$-\Delta\Delta H^{\ddagger}$, kcal mol^{-1}	$^{-}\Delta\Delta S^{\ddagger}$, cal mol^{-1} K^{-1}	$-\Delta\Delta G^{\ddagger}$(253 K), kcal mol^{-1}
Zr	4.4	6	2.9
Hf	4.6	8	2.6

For Zr and Hf catalysts, inversion at the metal has a higher enthalpic barrier than migratory insertion, and this difference is slightly more pronounced for the Hf complex while the inclusion of entropic factors leads to a reversal in $\Delta\Delta G^{\ddagger}$ for the two metals at, e.g., 253 K (i.e. inversion vs insertion for Zr is comparatively less facile than for Hf). In principle, if one knew the activation free energy for either process, this approach allows calculation of the other barrier. Recent experimental studies on propene insertion into metallocenium (or related) M−C bonds yield an indirect activation free energy of ca. 10−11 kcal mol^{-1} (depending on structure) at 253 K,[25] while inversion at the metal in another system of this type can be estimated at ca. 14.2 kcal mol^{-1} at this temperature.[26] It is gratifying to note that the difference in the barriers (3.2−4.2 kcal mol^{-1}) is more or less consistent with the results obtained here directly from the polymerization experiments.

A practical outcome for these types of complexes is that polymerization at lower temperatures and constant [M] should lead to more highly s-PP as Δ/[M] increases at lower temperatures (Table 5); that is, at lower temperatures one moves increasingly toward KQ conditions with both catalysts. We will demonstrate that the latter conclusion also applies to some more complicated, unsymmetrical systems discussed later.

A very interesting example related to these prototypical systems developed by Ewen and co-workers, are the doubly bridged zirconocene complexes (**3**) studied by Bercaw and co-workers.[14] These complexes show a wide range of polymerization behavior depending on the substituent R, producing s-PP when R is small and symmetrical, and i-PP when R is chiral and conforma-

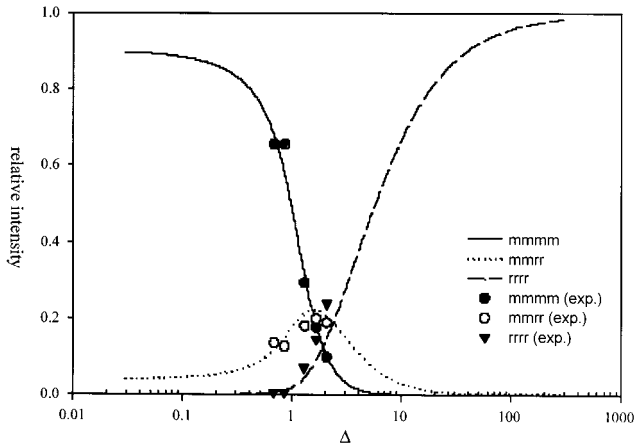

Figure 7. Diagnostic, normalized pentad intensities and theoretical fits vs Δ for PP prepared using catalyst **3** [R = CH(Me)^{t}Bu].

tionally "locked" and the polymerization is conducted at low [M]. Using the published pentad distribution data,[14] we can describe the behavior of the latter catalyst [**3**: R = CH(Me)^{t}Bu] as estimates for α (and β) are available from data using the symmetrical, doubly bridged complexes that are models for each state present.[14]

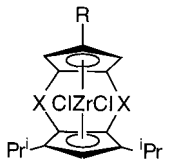

3: X = $SiMe_2$

In particular at lower [M] (Δ), this catalyst is operating in the C−H regime with $g/K = 40$, $\alpha = 0.99$, $\beta = 0.01$ (i.e., $\beta' = 0.99$ for the opposite enantioface) while at higher [M] (Δ), intermediate behavior is observed (Figure 7). The dramatic changes in the observed pentad distribution are brought about by extremely high and *opposing* stereoselectivities for insertion at each of the two iso-specific states, rather than by large changes in Δ. Interestingly, the magnitude of g/K suggests significant stability and/or reactivity differences between these two states in agreement with the conformational model proposed by Bercaw and co-workers.[14]

Model Application to C_1 *ansa*-Metallocene Catalysts. A series of polymerization experiments involving the simple, unsymmetrical, *ansa*-metallocene complexes $Me_2Y(Cp)(Ind)MCl_2$/MAO (Y = C, Si; M = Zr, Hf)[11] were conducted at a variety of [M] at 30 ± 1 °C and the results are summarized in Tables 6 (Y = C) and 7 (Y = Si). Under these carefully controlled conditions, it is evident that only the Me_2C-bridged, Hf complex exhibits significant changes in pentad distribution with [C_3H_6] (Table 6 and Figure 8).

The data obtained for this catalyst can be fit very well using the model (Figure 8) with $g/K = 9.0$, $\delta = 0.61$, $\alpha = 0.92$, and $\beta = 0.60$ (RSS < 0.005 for all pentads). The estimated parameters indicate that the rate constants for inversion and insertion from the B state are comparable (i.e., $\delta \sim 1$) while insertion from the isospecific state (A) is favored over inversion by a factor of ca. 5.5 at [M] = 1.0 M (i.e., $g/K \times \delta = k_p^A/k_1$). Moderately high stereoselectivity for the A state is predicted, and interestingly, the model also indicates that the B state is modestly stereoselective. We had earlier suggested that this might be true for the aspecific state in these catalysts as the *ansa*-indenyl ligand will exert some discrimination on propylene coordination and insertion.[11]

Table 6. Polymerization of Propylene Using $Me_2C(Cp)IndMCl_2$ Complexes and PMAO[a]

entry	M	[M] (μM)	[C_3H_6] (M)	T (°C)	R_p[b]	$M_w \times 10^3$	PDI	mmmm (%)[c]
1	Zr	20.0	1.30	30	20.2	1.7	2.70	12.2
2	Zr	20.0	2.21	30	34.8	1.9	2.70	13.7
3	Zr	20.0	3.26	30	52.0	2.0	3.00	12.4
4	Zr	5.00	8.82	30	6.0[d]	5.1	3.60	14.0
5	Hf	20.0	0.96	30	3.0	26.2	2.32	38.0
6	Hf	20.0	1.15	30	3.2	27.7	2.10	35.8
7	Hf	20.0	1.30	30	4.2	31.2	2.14	34.7
8	Hf	20.0	2.21	30	6.7	38.9	1.86	30.3
9	Hf	20.0	3.26	30	9.5	43.7	1.90	31.0
10	Hf	20.0	4.18	30	10.9	48.1	1.98	28.4
11	Hf	20.0	8.82	30	1.1[d]	43.2	1.98	23.0
12	Hf	20.0	3.61	10	1.6[d]	- -	- -	26.0
13	Hf	20.0	5.63	10	1.8[d]	70.8	3.25	26.5
14	Hf	20.0	8.72	10	2.4[d]	94.5	1.61	26.2

[a] Conditions: toluene (0.5 L), Al:M = 2000:1, ≥ 1000 rpm. [b] Steady-state rate of polymerization (mol of C_3H_6 mol^{-1} of M s^{-1}) as determined using calibrated mass flow meters except where noted. [c] The quoted intensities are precise to ±0.5% based on multiple integration of the same NMR spectrum while the error is ±1.5% based on multiple NMR spectra of the same polymer sample. [d] Polymerization activity in 10^5 g of PP/mol of M × h.

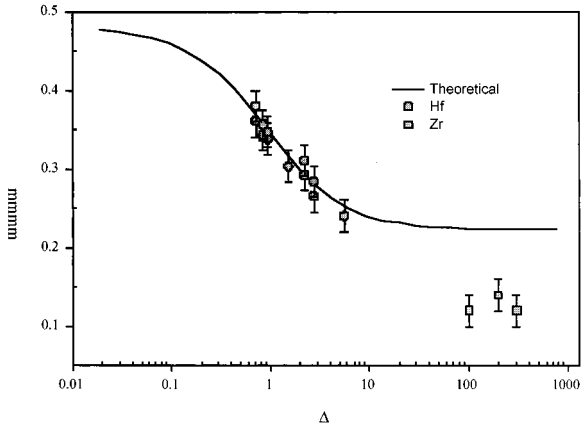

Figure 8. Theoretical mmmm pentad intensity (normalized to unity) vs Δ for $Me_2C(Cp)(Ind)MCl_2$/MAO with experimental points shown for both M = Hf (circles) and M = Zr (squares). The position of the latter points along the horizontal axis is entirely arbitrary except that $\Delta \gg 1$.

The model is reasonably well behaved although the maximum correlation coefficient is −0.95 for α and g/K. Thus, g/K and α are correlated, implying that essentially the same pentad distributions can be obtained by a linear increase in the reactivity/stability (g/K) followed by a corresponding decrease in the stereoselectivity (α) of the isospecific state. Ideally, one should have an independent method for estimating e.g. α in order to uniquely determine a value for g/K and β as asymptotic behavior is not exhibited by this complex (Figure 8).

Good estimates for α (and β) are available either through modeling of the transition structures involved[27] or from experimental data which may be available on the stereoselectivity of the first vs subsequent propylene insertions using an isosteric, C_2-symmetric metallocene complex as a model for the isospecific state in unsymmetric catalysts.[28]

However, as discussed above for Me_2C-bridged, C_s-symmetrical catalysts, operating at lower temperatures (and constant [M]) corresponds to conducting polymerization under conditions that approach kinetic quenching. In this regime, the pentad distribution is a function of α and β only and thus more reliable estimates for α (and β) can be obtained. With this in mind, polymerization experiments involving $Me_2C(Cp)(Ind)HfCl_2$/MAO were conducted at 10 °C and various [M] and the results are summarized in Table 6 (entries 12−14).

As can be seen from these results, the *mmmm* pentad intensity (and the pentad distribution) is now largely invariant to changes in [M] and with a microstructure that corresponds to that expected under KQ conditions. The best estimates for α and β at this lower temperature are $\alpha = 0.91 \pm 0.03$ and $\beta = 0.65 \pm 0.03$, respectively. These estimates are in good agreement with the ones made from data obtained at 30 °C and lend confidence to the values obtained for the other parameters at this temperature.

It is interesting to note that the values of α and β estimated at 30 °C are also in good agreement with those estimated for an isosteric, C_2-symmetric complex [i.e. $Me_2C(Ind)_2ZrCl_2$] from the pentad distribution and the stereoselectivity of the first monomer insertion, respectively.[28]

The asymptotic limit for the $Me_2C(Ind)(Cp)HfCl_2$/MAO catalyst in the KQ regime is shown in Figure 8 and it is evident that the more active Zr analogue produces PP with a pentad distribution which is not well described by the model with these same parameters and with $\Delta \gg 1$ over the entire concentration range as the experimental points do not lie on the theoretical curve of the Hf-based catalyst.[29] Actually, the best fit of the model (RSS < 0.02 for all pentads which is about four to five times worse than the fit obtained for the other catalysts studied—see Supporting Information) to the pentad data for the Zr catalyst corresponds to a case in which the isospecific state is much less stereoselective ($\alpha = 0.81$) and the stereoselectivity of the aspecific state also decreases ($\beta = 0.56$) and that KQ conditions pertain.

It should be pointed out that this complex produces oligomeric PP under all conditions (maximum $DP_n = 34$ in liquid propylene). It seems unlikely in this case that one can model the pentad distribution properly without taking into account chain-transfer processes involving the two states (i.e., the rate of formation of a polymer chain is comparable to the rate of pentad formation so the steady-state approximation relating to *n*-ad formation may not be valid) so the parameters estimated from the pentad distribution are probably in error.

In the case of the Me_2Si-bridged systems, one is faced with a problem. Neither of these catalysts produce PP where the pentad distributions show any strong dependency on [C_3H_6] (Table 7), yet the average stereoregularity of the PP is clearly different and higher for Hf vs Zr. While it might be tempting to invoke C−H behavior for the Hf complex and KQ behavior for the Zr-analogue,[9b] the absolute changes required in Δ (i.e., 10^3) are unreasonable within the context of a 5−10-fold difference in activity (Table 7).

In fact, the observed pentad distributions are well described (RSS < 0.005) if both catalysts function within the C−H regime with $\bar{\epsilon} = 0.800$ for Zr and $\bar{\epsilon} = 0.875$ for Hf but the fundamental parameters, *g*/*K*, δ, α, and β are different for each.[30] There are an infinite number of solutions that will fit the data in this regime as the model parameters are highly correlated and so no direct mechanistic information is available solely through the analysis of the pentad distribution.

Table 7. Polymerization of Propylene Using $Me_2Si(Cp)IndMCl_2$ Complexes and PMAO[a]

entry	M	[M] (μM)	[C_3H_6] (M)	R_p[b]	M_w (K)	PDI	mmmm (%)[c]
1	Zr	5.0	8.82	51[d]	19.3	2.20	33.8
2	Zr	2.5	4.18	233	18.7	2.10	34.9
3	Zr	2.5	3.26	209	14.9	1.77	33.8
4	Zr	2.5	2.21	135	13.3	1.77	31.4
5	Zr	2.5	1.15	49.6	11.6	1.70	31.4
6	Hf	20.0	4.18	23.5	200	2.25	49.6
7	Hf	20.0	3.26	18.9	188	2.81	52.2
8	Hf	20.0	2.21	14.4	152	2.02	51.8
9	Hf	20.0	1.30	8.8	100	1.70	51.2
10	Hf	20.0	1.15	7.5	99.1	2.16	51.4
11	Hf	20.0	0.96	4.8	91.1	2.36	51.7

[a] Conditions: toluene (0.5 L), Al:Zr = 1000:1, Al:Hf = 2000:1, ≥1000 rpm. [b] Steady-state rate of polymerization (mol of C_3H_6 mol^{-1} of M s^{-1}) as determined using calibrated mass flow meters except where noted. [c] The quoted intensities are precise to ±0.5% based on multiple integration of the same NMR spectrum while the error is ±1.5% based on multiple NMR spectra of the same polymer sample. [d] Polymerization activity in 10^5 g of PP/mol of M × h.

If we assume that the value of *g*/*K* estimated from the pentad distributions for the Me_2C-bridged Hf complex (*g*/*K* = 9.0) is unaffected in the Me_2Si-bridged catalysts,[31] one can use eq 6 to calculate that $\alpha = 0.91_7$ for Hf and 0.83_3 for Zr for $\beta = 0.5$ or that $\alpha = 0.90_6$ for Hf (with $\beta = 0.60$) and 0.82_7 for Zr (with $\beta = 0.56$—vide supra). While these values are (fortuitously) close to those estimated for the Me_2C-bridged Hf and Zr complexes above, it is well-known, at least in isospecific polymerization, that Me_2Si-bridged catalysts are significantly more stereoregulating than their C-bridged analogues.[28] This suggests that $g/K \leq 9.0$ for the Me_2Si-bridged complexes but without additional information we cannot make further progress through modeling of these systems.[32]

Conclusions

The kinetic model described here can account for the diverse behavior exhibited by *ansa*-metallocene complexes and can be used to extract fundamental parameters of interest from polymer microstructure, especially where the pentad distribution responds to changes in monomer concentration. Even in cases where the pentad distribution is invariant to changes in [M], it is possible to distinguish between C−H and KQ conditions with a reasonable degree of certainty.

For simple systems, where *g*/*K* is known with certainty from symmetry considerations, reliable conclusions about differential behavior between catalysts can be made. Unfortunately, for unsymmetrical systems, good estimates for fundamental parameters requires that one study catalysts which operate in the intermediate regime. We have been able to make educated guesses about the behavior of two systems operating under C−H conditions, but clearly additional information would be required for unambiguous estimation of *g*/*K*, α and β.

It is interesting that substitution of a Me_2Si for a Me_2C bridge in these complexes has such a significant effect on the rate of inversion vs insertion. For example, as the results in Tables 6 and 7 indicate, the Me_2Si-

bridged Hf complex is about 2 × more active than its Me_2C-bridged counterpart under equivalent conditions so the fact that the former complex functions at *lower* absolute values of Δ implies that inversion at the metal center is proportionately much faster (i.e., by at least a factor of 20 assuming equal and efficient activation of both pre-catalysts by MAO).

Similar observations seem to also pertain to Me_2Si- vs Me_2C-bridged complexes that form s-PP; as has been documented elsewhere,[33] the former complexes furnish s-PP of much lower stereoregularity under equivalent conditions than the latter, suggesting a higher rate of chain inversion.

The factors which could influence the rate of this inversion process include the nature of the counterion (i.e., more strongly coordinating counterions are known to hinder ion-pair reorganization processes that involve inversion at the metal[6]), presumably solvent polarity for similar reasons,[7] and/or metallocene structure.

Considerably less theoretical and experimental attention has been devoted to this latter aspect.[26] A simple steric argument would seem to indicate the *opposite* conclusion—i.e., that the Me_2C-bridged systems should feature comparatively faster inversion rates as the carbon atoms of a metal alkyl group are further away from the *ansa*-ligand in these complexes.[11] However, by this same argument, counterion effects would be consistent with the observed trend—i.e., a more strongly associated counterion should hinder inversion at the metal in the Me_2C-bridged catalysts. Future work will focus on the study of this issue; in particular, counterion effects on PP microstructure manifest themselves in fairly subtle ways depending on the relevant kinetic regime for unsymmetrical complexes.[6b,31]

Experimental Section

Detailed experimental procedures for preparation of complexes **1** and **2** as well as unsymmetrical catalysts $Me_2Y(Cp)(Ind)MCl_2$ (Y = C, Si; M = Zr, Hf) have been published elsewhere.[3,11] Propylene polymerization in toluene solvent and characterization of poly(propylene) involved techniques and methods that have presented in detail elsewhere.[9,11] Propylene solubilities in toluene as a function of *P*,T were estimated from literature data[34] or from empirical equations[9] and appear in Tables 4, 6, and 7. Mass transfer limitations can significant affect PP MWD and microstructure even using single site catalysts if the polymer formed is soluble in the reaction medium;[8] diffusion-limited, polymerization experiments in toluene can be detected by variation in monomer flow with, e.g., stirring speed. All polymerization experiments reported here were conducted at catalyst concentrations and at stirring speeds (≥1000 rpm) such that intrinsic behavior was studied. All pentad modeling studies were executed using an IBM-PC and software programs locally written in Fortran.[17]

The following is a typical experimental procedure for liquid propylene polymerization: A 1.0 L reactor was charged with ca. 0.5 L of liquid propylene by condensing the gas at 80−100 psi into the reactor at −15 °C and using a calibrated mass flow controller to monitor/control flow during this period. After the requisite amount of monomer had been condensed, the propylene flow was shut off and the reactor warmed to the process temperature. A solution of PMAO−IP in toluene (ca. 10−15 mL), corresponding to half of the total PMAO used, was introduced into the reactor via an over-pressurized, stainless steel sample vessel, and the reactor and contents were conditioned by vigorous stirring for at least an hour prior to catalyst introduction. A solution of the metallocene complex and the remainder of the MAO in toluene (15−10 mL or 25 mL total) were then introduced via an over-pressurized sampling vessel to initiate polymerization.

Polymerizations were halted by adding 2-propanol (25 mL) via over-pressurized sampling vessel and the reactor carefully vented. Toluene solvent was used to rinse the polymer solution/slurry into a round-bottom flask through a bottom drain valve in the reactor and the solvent was then removed in vacuo to isolate the polymer product, obtained as either a gummy wax or rubbery solid in the case of elastomeric PP or a semicrystalline powder in the case of s-PP.

Catalyst/aluminoxane residues were removed from elastomeric PP samples by Soxhlet extraction of the polymer with refluxing toluene and the purified polymeric extracts were again concentrated in vacuo or by evaporation at atmospheric pressure to obtain purified polymer which was then characterized as described elsewhere.[9,11] Syndiotactic PP samples were de-ashed by washing with MeOH, 6 N HCl-MeOH and then MeOH prior to drying in vacuo at 60 °C and 0.01 mmHg.

Acknowledgment. The authors would like to thank the Natural Sciences and Engineering Research Council of Canada, Conselho Nacional de Pesquisa of Brazil, Nova Chemicals Corp. of Calgary, Alberta, Canada, and Polibrasil Resinas S.A. of Sao Paulo-SP, Brazil, for financial support of this work. The technical assistance of Drs. Yuding Feng and Xiarong Jin in obtaining SEC and DSC analyses of some of the polymer samples prepared here is gratefully acknowledged.

Supporting Information Available: Text and tables giving mathematical formulation of the model and derivation of expressions governing MW, block length and stereosequence distributions, representative experimental and calculated pentad intensities for PP prepared with $Me_2Y(Cp)(Ind)MCl_2$/PMAO catalysts (Y = C, Si; M = Zr, Hf). This material is available free of charge via the Internet at http://pubs.acs.org.

References and Notes

(1) For reviews on metallocene-catalyzed propylene polymerization, see: (a) Coates, G. W. *Chem. Rev.* **2000**, *100*, 1223. (b) Resconi, L.; Cavallo, L.; Fait, A.; Piemontesi, F. *Chem. Rev.* **2000**, *100*, 1253. (c) Brintzinger, H.-H.; Fischer, D.; Mulhaupt, R.; Rieger, B.; Waymouth, R. M. *Angew. Chem., Int. Ed. Engl.* **1995**, *34*, 1143.

(2) (a) Ewen, J. A. *J. Am. Chem. Soc.* **1984**, *106*, 6355. (b) Kaminsky, W.; Kulper, K.; Brintzinger, H.-H.; Wild, F. W. R. P. *Angew. Chem., Int. Ed. Engl.* **1985**, *24*, 507.

(3) (a) Ewen, J. A.; Jones, R. L.; Razavi, A.; Ferrara, J. D. *J. Am. Chem. Soc.* **1988**, *110*, 6255. For some recent mechanistic/theoretical work on syndiospecific polymerization catalysts, see: (b) Grisi, F.; Longo, P.; Zambelli, A.; Ewen, J. A. *J. Mol. Catal. A: Chem.* **1999**, *140*, 225. (c) Ewen, J. A. *J. Mol. Catal. A: Chem.* **1998**, *128*, 103.

(4) (a) Ewen, J. A.; Elder, M. J. *Makromol. Chem., Makromol. Symp.* **1993**, *66*, 179. (b) Llinas, G. H.; Day, R. O.; Rausch, M. D.; Chien, J. C. W. *Organometallics* **1993**, *12*, 1283.

(5) Mallin, D. T.; Rausch, M. D.; Lin, G.-Y.; Dong, S.; Chien, J. C. W. *J. Am. Chem. Soc.* **1990**, *112*, 2030.

(6) (a) Chen, Y.-X.; Metz, M. V.; Li, L.; Stern, C. L.; Marks, T. J. *J. Am. Chem. Soc.* **1998**, *120*, 6287. (b) Giardello, M. A.; Eisen, M. S.; Stern, C. L.; Marks, T. J. *J. Am. Chem. Soc.* **1995**, *117*, 12114.

(7) (a) Chien, J. C. W.; Song, W.; Rausch, M. D. *J. Polym. Sci., Part A: Polym. Chem.* **1994**, *32*, 2387. (b) Herfert, N.; Fink, G. *Makromol. Chem.* **1992**, *193*, 773.

(8) A kinetic model for use with fluxional catalysts has also been developed: Nele, M.; Collins, S.; Pinto, J. C.; Diaz, M.; Lin, S.; Waymouth, R. M. *Macromolecules* **2000**, *33*, 7249.

(9) (a) Bravakis, A. M.; Bailey, M. P.; Pigeon, M.; Collins, S. *Macromolecules* **1998**, 31, 1000. (b) Mohammed, M.; Xin, S.; Collins, S. *Am. Chem. Soc. PMSE Prepr.* **1999**, *80*, 441.

(10) Ewen, J. A.; Elder, M. J.; Jones, R. L.; Haspelagh, L.; Atwood, J. L.; Bott, S. G.; Robinson, K. *Makromol. Chem., Makromol. Symp.* **1991**, *48/49*, 253.

(11) (a) Gauthier, W. J.; Corrigan, J. F.; Taylor, N. J.; Collins, S. *Macromolecules* **1995**, *28*, 3771. (b) Gauthier, W. J.; Collins, S. *Macromolecules* **1995**, *28*, 3779.

(12) See, inter alia: (a) Kleinschmidt, R.; Reffke, M.; Fink, G. *Macromol. Rapid Commun.* **1999**, *20*, 284. (b) Dietrich, U.; Hackmann, M.; Rieger, B.; Klinga, M.; Leskela, M. *J. Am. Chem. Soc.* **1999**, *121*, 4348. (c) Rieger, B.; Jany, C.; Fawzi, R.; Steimann, M. *Organometallics* **1994**, *13*, 647.
(13) (a) Farina, M.; DiSilvestro, G.; Sozzani, P. *Macromolecules*, **1993**, *26*, 946. (b) DiSilvestro, G.; Sozzani, P.; Terragni, A. *Macromol. Chem. Phys.* **1996**, *197*, 3209. (c) Farina, M.; DiSilvestro, G.; Terragni, A. *J. Am. Chem. Soc.* **1995**, *196*, 353.
(14) This model was briefly mentioned in the following paper: Veghini, D.; Henling, L. M.; Burkhardt, T. J.; Bercaw, J. E. *J. Am. Chem. Soc.* **1999**, *121*, 564, ref 26.
(15) De Carvalho, A. B. M.; Gloor, P. E.; Hamielec, A. E. *Polymer* **1990**, *31*, 1290.
(16) (a) Shelden, R. A.; Fueno, T.; Tsunetsugu, T.; Furukawa, J. *J. Polym. Sci., Polym. Lett. Ed.* **1965**, *3*, 23. (b) Bovey, F. A.; Tiers, G. V. D. *J. Polym. Sci.* **1960**, *44*, 173.
(17) Nele, M. Ph.D. Thesis, Universidade Federal do Rio de Janeiro, 2000.
(18) We thank a reviewer for reminding us of the mechanistic complexity of most propylene polymerizations using metallocene catalysts.
(19) While lower concentrations are accessible, one should bear in mind that many metallocene complexes function as epimerization catalysts at sufficiently low [M] and this process would obviously degrade any intrinsic stereoregulation. (a) Busico, V.; Cipullo, R.; Caporaso, L.; Angelini, G.; Segre, A. L. *J. Mol. Catal. A: Chem.* **1998**, *128*, 53. (b) Busico, V.; Brita, D.; Caporaso, L.; Cipullo, R.; Vacatello, M. *Macromolecules* **1997**, *30*, 3971. (c) Borriello, A.; Busico, V.; Cipullo, R.; Fusco, O.; Chadwick, J. C. *Macromol. Chem. Phys.* **1997**, *198*, 1257. (d) Busico, V.; Caporaso, L.; Cipullo, R.; Landriani, L.; Angelini, G.; Margonelli, A.; Segre, A. L. *J. Am. Chem. Soc.* **1996**, *118*, 2105. (e) Leclerc, M. K.; Brintzinger, H. H. *J. Am. Chem. Soc.* **1996**, *118*, 9024. (f) Busico, V.; Cipullo, R. *J. Organomet. Chem.* **1995**, *497*, 113−118. (g) Leclerc, M. K.; Brintzinger, H. H. *J. Am. Chem. Soc.* **1995**, *117*, 1651. (h) Resconi, L.; Fait, A.; Piemontesi, F.; Colonnesi, M.; Rychlicki, H.; Zeigler, R. *Macromolecules* **1995**, *28*, 6667. (i) Busico, V.; Cipullo, R. *J. Am. Chem. Soc.* **1994**, *116*, 9329.
(20) (a) Cheng, H. N.; Babu, G. N.; Newmark, R. A.; Chien, J. C. W. *Macromolecules* **1992**, *25*, 6980. (b) Cheng, H. N.; Babu, G. N.; Newmark, R. A.; Chien, J. C. W. *Macromolecules* 7400.
(21) On the other hand, for oligomers it should be possible to do this if they are sufficiently low MW to be detected by mass spectrometry.
(22) (a) Collete, J. W.; Tullock, C. W.; MacDonald, R. N.; Buck, W. H.; Su, A. C. L.; Harrel, J. R.; Mulhaupt, R.; Anderson, B. C. *Macromolecules* **1989**, *22*, 3851. (b) Collete, J. W.; Ovenall, D. W.; Buck, W. H.; Ferguson, R. C. *Macromolecules* 3858.
(23) (a) Hanna, S.; Windle, A. H. *Polymer* **1988**, *29*, 207. (b) Tarek, M. M.; Mark, J. E. *J. Appl. Polym. Sci., Part B: Polym. Phys.* **1997**, *35*, 2757. (c) Tarek, M. M.; Mark, J. E. *Macromol. Theory Simul.* **1998**, *7*, 69.
(24) Ewen, J. A.; Elder, M. J.; Jones, R. L.; Curtis, S.; Cheng, H. N. Catalytic Olefin Polymerization. In *Studies in Surface Science Catalysis*; Keii, T., Soga, K., Eds.; Elsevier: Amsterdam, 1990; Vol. 56.
(25) Dahlmann, M.; Erker, G.; Bergander, K. *J. Am. Chem. Soc.* **2000**, *122*, 7986 and references therein.
(26) Casey, C. P.; Carpenetti II, D. W. *Organometallics* **2000**, *19*, 3970 and references therein.
(27) For recent reviews, consult: (a) Rappe, A. K.; Skiff, W. M.; Casewit, C. J. *Chem. Rev.* **2000**, *100*, 1435. (b) Angermund, K.; Fink, G.; Jensen, V. R.; Kleinschmidt, R. *Chem. Rev.* **2000**, *100*, 1457.
(28) (a) Resconi, L.; Piemontesi, F.; Camurati, I.; Sudmeijer, O.; Nifant'ev, I. E.; Ivchenko, P. V.; Kuz'mina, L. G. *J. Am. Chem. Soc.* **1998**, *120*, 2308. (b) Sacchi, M. C.; Barsties, E.; Tritto, I.; Locatelli, P.; Brintzinger, H.-H.; Stehling, U. *Macromolecules* **1997**, *30*, 3955.
(29) The position of these data points along the Δ scale is entirely arbitrary although this catalyst does function under KQ conditions.
(30) Attempts to model the pentad distribution for either catalyst assuming KQ conditions pertain led to a solution where $\alpha = \beta$ and the correlation coefficient between these two parameters was unity (see Supporting Information for details).
(31) NMR studies have revealed little difference in the relative stability (i.e. K) of isomeric ion-pairs derived from $Me_2Y(Cp)IndMMe_2$ (Y = C, Si, M = Zr, Hf) and $B(C_6F_5)_3$: Mohammed, M.; Xin, S.; Nele, M. N.; Collins, S. manuscript in preparation.
(32) The temperature-dependent behavior of $Me_2Si(Cp)IndHfCl_2$ was examined (10 and 50 °C); although overall polymer tacticity increases slightly at lower temperatures (and constant [M]), the pentad distribution was still invariant to changes in [M] at a particular temperature. Mohammed, M. Unpublished observations.
(33) Chen, Y.-X.; Rausch, M. D.; Chien, J. C. W. *J. Organomet. Chem.* **1995**, *497*, 1.
(34) (a) Atiqullah, M.; Hammawa, H.; Hamid, H. *Eur. Polym. J.* **1998**, *34*, 1511. (b) Reid, R. R.; Prausnitz, J. M.; Poling, B. E. *The Properties of Gases & Liquids*; McGraw-Hill: Singapore, 1987.

MA0021186